

Structure-factor measurements in ^4He as a function of density

H. N. Robkoff and R. B. Hallock

*Laboratory for Low Temperature Physics, Department of Physics and Astronomy,
University of Massachusetts, Amherst, Massachusetts 01003*

(Received 3 August 1981)

Measurements of the structure factor $S(k)$ for ^4He are reported as a function of pressure at 1.67, 2.20, and 4.24 K from saturated vapor pressure to 25 atm. The liquid structure factor is seen to sharpen and increase in amplitude with an increase in pressure at each of the temperatures studied. Comparison is made to previous results obtained by the technique of neutron scattering as well as to the theoretical predictions of Chang and Campbell and of Whitlock *et al.* The pair correlation function $g(r)$ is obtained from the liquid structure factor by means of a Fourier transform, and comparison is made to theoretical predictions.

I. INTRODUCTION

The structure of liquid helium has been a subject of continuing interest since the original diffraction experiments of Keesom and Taconis.¹ These and subsequent early experiments were designed to search for long-range order and to test the ideas of Frolich² concerning a possible diamond lattice in the superfluid state and its disappearance during the transition to the normal state. In the intervening years there has been a shift of emphasis away from the transition region and toward experiments of higher accuracy so as to provide detailed tests for the theories of the ground state. Very recently there has again been a focus on the transition region^{3,4} where clear spatial order changes associated with the λ transition have been confirmed. There remains a need for systematic data as a function of density at fixed temperature. This is particularly true in light of the recent theoretical work of Chang and Campbell,⁵ Whitlock *et al.*,⁶ and Gaglione *et al.*⁷ It is this need to which the current work is addressed.

We report here measurements of the liquid structure factor $S(k)$ as a function of momentum transfer, k , as a function of pressure along the three isotherms 1.67, 2.20, and 4.24 K. Particular attention is paid to the small momentum transfer region $k \leq 0.9 \text{ \AA}^{-1}$ and to the region of the principal structure factor maximum although the full data set covers the momentum transfer interval $0.2 \leq k \leq 5.2 \text{ \AA}^{-1}$. In general the small momentum transfer results agree with expectations based on thermodynamics in the limit of vanishing momentum transfer. In the region of the principal structure factor maximum we document the increase in spatial order as a function of increasing density.

In Sec. II we present a brief discussion of the liquid structure factor and the pair correlation function and describe relevant theoretical work. Section III con-

tains a limited discussion of the apparatus. A more detailed description may be found elsewhere.^{8,9} The results for $S(k)$ and $g(r)$ are presented in Sec. IV as is a comparison to previous work and relevant theory. A brief summary appears in Sec. V.

II. LIQUID STRUCTURE FACTOR

The diffraction pattern observed in an x-ray scattering experiment is due to a number of factors but one of the most important is the spatial arrangement of the atoms in the sample under investigation. This spatial arrangement is reflected in the pair correlation function $g(\vec{r})$ which gives the probability (normalized to unity at large values of $|\vec{r}|$) of finding an atom at position \vec{r} if it is known that an atom resides at the origin. In the case of an isotropic, monatomic liquid such as helium $g(\vec{r})$ is isotropic and hence one has $g(\vec{r}) \equiv g(r)$ where r is the distance between the two atoms in question. The pair correlation function is often directly available from theories of the liquid state.

Measurements of $g(r)$ proceed by way of the liquid structure factor since it is this which is directly measured in a diffraction experiment. The intensity observed as a function of momentum transfer in a scattering experiment can be written as¹⁰

$$I(k) = ANT[\sigma_e S(k) + \sigma_i] \quad (1)$$

Here A is the Thompson scattering from a single electron, σ_e and σ_i are, respectively, the coherent and incoherent scattering factors which account for the fact that the scatter from the two electrons within a helium atom is not independent, N accounts for the fact that a given sample has many atoms which can participate in the scattering and T is a transmission

factor necessary since the main x-ray beam has been attenuated before it can interact with atoms deeper in the sample. The liquid structure factor, $S(k)$, modulates the scattered intensity because there is constructive or destructive interference in the scattered radiation as a result of spatial correlations among the atoms.

Formally the liquid structure factor is related to these correlations by a Fourier transform

$$S(k) = 1 + \rho \int e^{i\vec{k}\cdot\vec{r}} [g(r) - 1] d^3r, \quad (2)$$

where ρ is the density of the liquid helium under study. The approach of this work is to obtain values for the liquid structure factor through use of Eq. (1) and the pair correlation function through the inverse of Eq. (2).

Theoretical predictions relevant to the present work are few since it has been only recently that detailed attention has been paid to the density dependence of the ${}^4\text{He}$ ground state. Theoretical calculations for several densities have been reported by Chang and Campbell⁵ for the ground state. In their work, results for the liquid structure factor are obtained from an optimum Jastrow function by multiple iteration of the paired phonon analysis. The final result is observed to be independent of the initial guess for the trial function. The minimization procedure requires a computation of the energy and Chang and Campbell⁵ accomplish this by means of the hypernetted-chain approximation.¹¹ For a given choice of potential this procedure results in the best variational calculation available within the context of Jastrow functions. Two potentials, the Lennard-Jones (LJ) and the Morse-dipole-dipole (MDD2), were used in separate calculations and detailed results for the liquid structure obtained for both. More recently Whitney and Campbell¹² have extended these calculations to several other potentials. In addition work on the inclusion of three-body factors was completed⁵ as a first step in enlarging the class of functions beyond the Jastrow form. In general the inclusion of such factors results in somewhat sharper structure in $S(k)$ and improved agreement with experiment.

More recently Whitlock *et al.*⁶ have completed a detailed study of the Lennard-Jones system with the de Boer–Michels¹³ parameters as appropriate for ${}^4\text{He}$ by use of the Green's-function Monte Carlo method. The advantages of this method include the fact that it is possible to compute exactly the ground-state energy of the system with the potential chosen for study. The pair correlation function is computed by means of a reliable extrapolation technique and the liquid structure factor is obtained by a Fourier transformation of the pair correlation function.

III. APPARATUS AND PROCEDURE

The apparatus used for the present work is essentially the same as that used for our earlier studies at saturated vapor pressure.⁸ A detailed discussion of the apparatus is available elsewhere⁹ and only a brief account is necessary here. Copper $\text{Cu } K\alpha$ radiation of nominal wavelength 1.54 Å is generated in a Rigaku¹⁴ RU-200PL rotating anode x-ray source and is scattered from a cylindrical target of 9.5-mm diameter. The scattering chamber has a wall thickness of 0.25 mm and is machined from beryllium of low iron content. The scattered x rays are detected by means of an energy sensitive intrinsic germanium device with an energy resolution of 280 eV. This allows monochromatization to be done at the detection stage where attention is focused on $\text{Cu } K\alpha$ x rays. Vertical and horizontal resolution of the diffractometer is measured to be 0.3° or about 0.04 \AA^{-1} .

As has been described previously,^{8,9} the diffractometer incorporates monitor counting devices to correct for main beam intensity changes during the course of the measurements. In addition the data are self-consistently normalized by reference to repeated data sets with the same temperature and pressure which are interspersed throughout the course of the complete data collection.

The target samples of helium are liquified from high purity gas¹⁵ and allowed to stabilize at the selected temperature and pressure for at least an hour prior to data collection. Temperature is measured by reference to a calibrated germanium resistance thermometer¹⁶ and pressures are measured by means of a temperature compensated Heise gauge which has been tested against a dead weight pressure gauge and found to be accurate to ± 1 psi over its entire 0–600-psi range.

To obtain the structure factor of interest from the observed intensity requires the use of Eq. (1). This cannot be done directly due to the impossibility of counting the precise number of atoms N which act as target atoms. Rather, in a second measurement in the same apparatus, scattering is observed from neon at 77 K and 1 atm pressure for which $S(k) = 1$ to within 0.4% for all momentum transfer values of interest. The ratio of two equations of the form of Eq. (1) is then formed^{17,18} and $N_{\text{He}}/N_{\text{Ne}}$ is eliminated in favor of $\rho_{\text{He}}/\rho_{\text{Ne}}$ since $N = \rho V$ for each substance. Here ρ is the number density of the target material and V is the target volume which is the same in each case. The liquid structure factor for helium is thus determined in terms of the ratio of two measured scattering intensities the known scattering factors for helium¹⁹ and neon²⁰ and the transmission factors²¹ and number densities.^{22–24} In the case of neon the densities were computed from the virial equation using the second virial coefficient as given by Dymond and Smith.²⁵ Other factors such as multiple scatter-

ing corrections have also been considered in the manner previously reported.⁸

The structure factor values reported here has been forced to unity at large values of the momentum transfer,⁸ a procedure which required no more than a 5% correction at the largest momentum transfer values in most cases and usually considerably less. The imposition of this physical condition on the data is sensible but was necessary in our case due to difficulties, we suspect, with the main beam intensity⁸

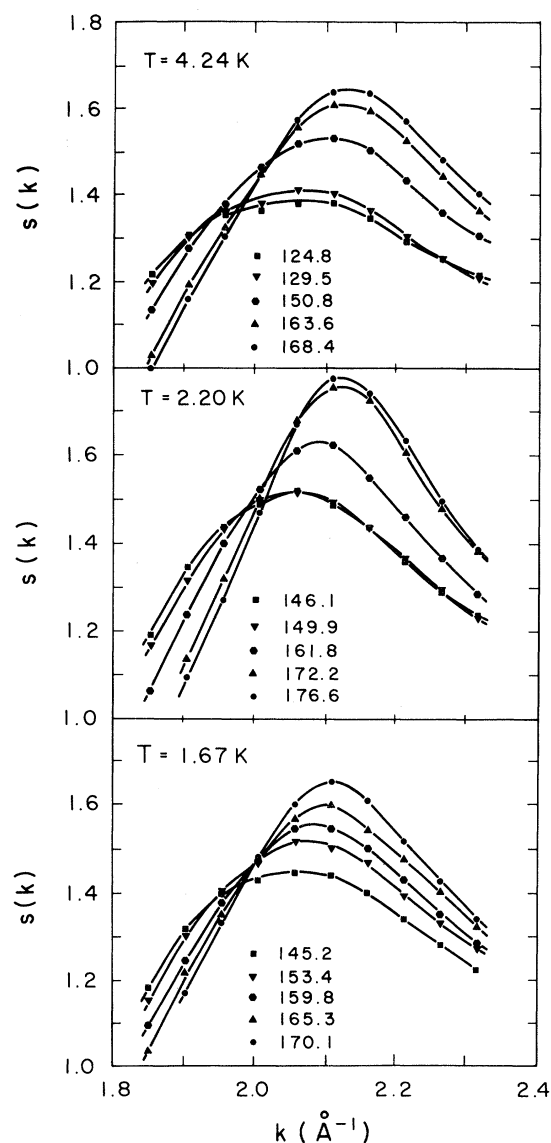


FIG. 1. Experimental liquid structure values obtained in this work in the vicinity of the principal structure factor maximum. The smooth curves drawn through the data are guides to the eye and do not represent any theory. The numbers beside the symbol identification refer to the density in kg/m^3 .

which was observed to slowly decrease between x-ray tube filament changes. The effect of this procedure in the region of the principal structure factor peak is no larger than 0.3%. As we have discussed in detail previously,⁸ the overall errors in this work are about 4% although the difference between two structure factor values is known to considerably greater confidence, perhaps 1%.

IV. RESULTS

The liquid structure factor has been determined at five densities along each of the isotherms 1.67, 2.20, and 4.24 K. A numerical tabulation of the results is presented in the Appendix. In general the structure factor is observed to behave with an increase in density in a manner consistent with previous observations by others. That is, the principal structure factor maximum is observed to increase and grow sharper with an increase in the density. The location of the maximum is also observed to move smoothly to larger values of momentum transfer as the density is increased. This behavior is illustrated in Figs. 1 and 2. In Fig. 1 the raw $S(k)$ values as obtained in this

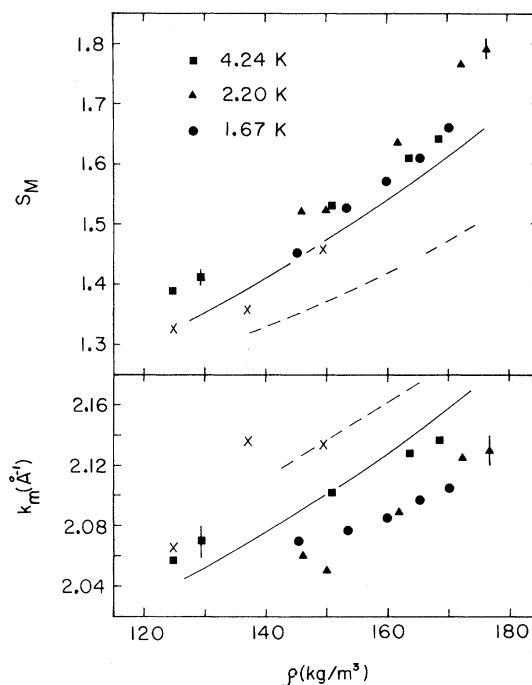


FIG. 2. The height S_M and position k_m of the principal structure factor maximum as a function of density for each of the temperatures studied. The lines are from the work of Chang and Campbell (Ref. 5) including three-body factors for the Lennard-Jones (dashed lines) and Morse MDD2 (solid lines) potentials. The crosses are the Monte Carlo predictions of Whitlock *et al.* (Ref. 6) for the Lennard-Jones potentials. Both theoretical works are $T=0$ K calculations.

work are presented. The smooth curves drawn through the data points are merely guides to the eye and have no other significance. The maximum value of $S(k)$, S_M , and the location of the maximum in momentum transfer k_m are shown for each temperature as a function of density in Fig. 2. Also shown in Fig. 2 are the theoretical predictions of Chang and Campbell⁵ for the case of the Lennard-Jones (dashed line) and the Morse (solid line) potentials for the case where three-body factors have been included in the calculation. The Morse potential is seen to be in better agreement with the data than is the Lennard-

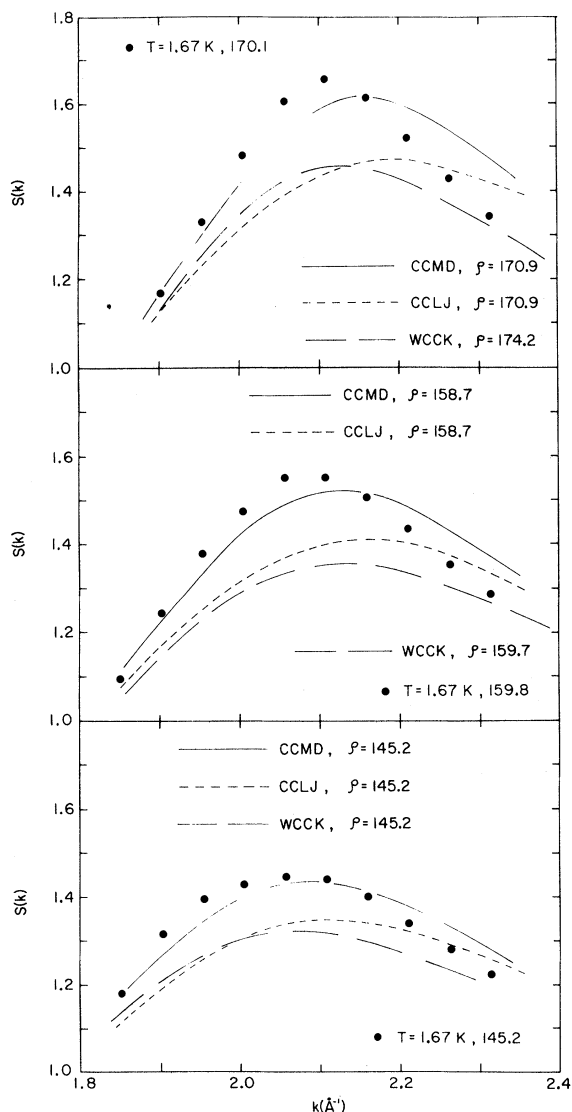


FIG. 3. Comparison of the experimental structure factors at 1.67 K and three densities with the $T=0$ K calculations of Chang and Campbell (Ref. 5) and Whitlock *et al.* (Ref. 6). In the work of Chang and Campbell we have selected the three-body calculations for comparison.

Jones. This preference for the Morse potential over the Lennard Jones is consistent with earlier work⁸ at saturated vapor pressure. Also shown on Fig. 2 are the predictions of Whitlock *et al.*⁶ based on a Monte Carlo calculation with the Lennard-Jones potential.

The comparison between the experimental results and the theoretical predictions is more fully presented in Fig. 3 where the general agreement with the Morse potential is clear. Again here the predictions of Chang and Campbell⁵ are those which include three body factors.

Data at small momentum transfer are shown in Fig. 4 for each of the temperatures and densities stud-

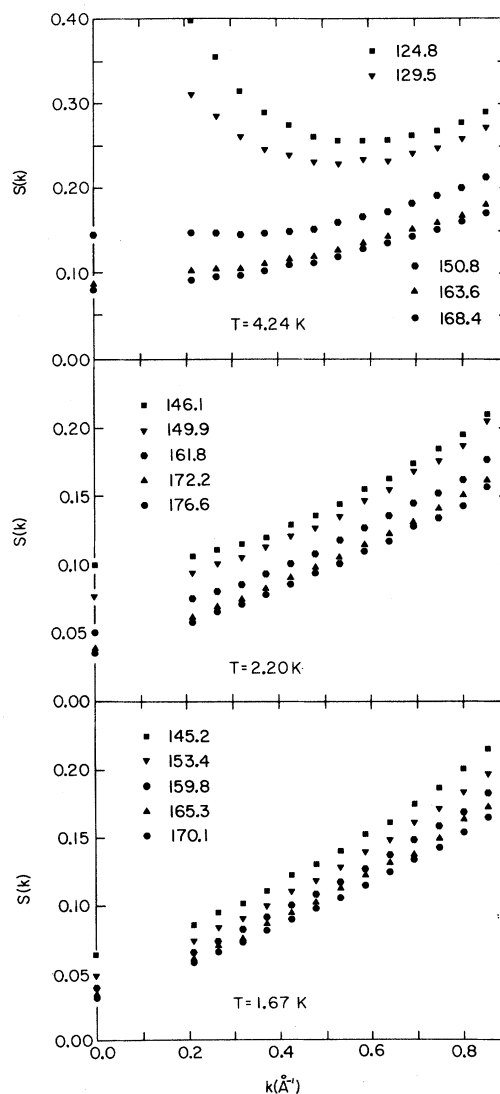


FIG. 4. Experimental liquid structure factor values for small momentum transfer. The intercepts at $k=0$ are obtained from Eq. (3). The density values in kg/m^3 are shown beside the appropriate symbols.

ied in this work. The data generally extrapolate smoothly to the zero momentum transfer limit

$$S(0) = \lim_{k \rightarrow 0} S(k) = \rho k_B T X_T = \frac{\gamma k_B T}{mc^2}, \quad (3)$$

where ρ is the density, k_B the Boltzmann constant, T the temperature, X_T the isothermal compressibility, γ the ratio of specific heats, m the mass of a helium atom, and c the velocity of ordinary sound. The $S(k)$ values shown on the intercept in Fig. 4 have been computed from the right side of Eq. (3) using known values of γ and c . The expected quadratic²⁶ dependence of $S(k)$ as a function of k for small values of the momentum transfer is consistent with but not confirmed by the present data.

Data to which the present results as a function of density can be compared are sparse. Henshaw²⁷ carried out an extensive series of measurements at various temperatures and densities but did not publish²⁷ complete tables of the structure factor values. Nonetheless, comparison to his work can be made through use of the function

$$f(k) = \frac{2}{\pi} k [S(k) - 1] \quad (4)$$

and this comparison is presented in Fig. 5 where the

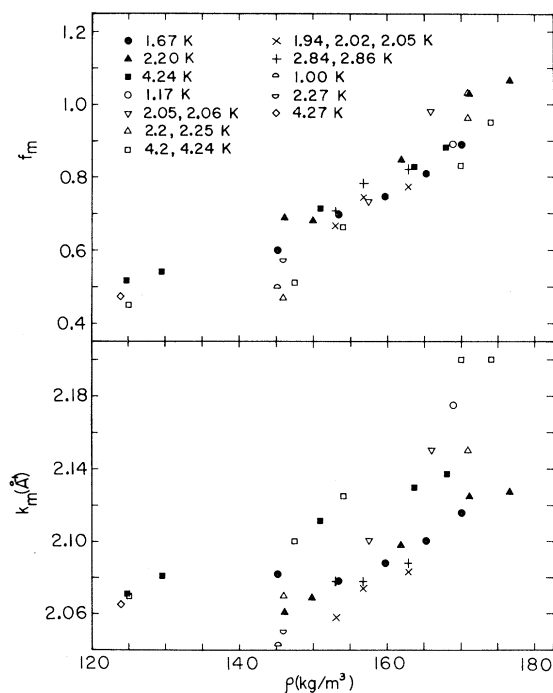


FIG. 5. The maximum value f_m and location k_m , of the function, $f(k) = 2k[S(k) - 1]/\pi$ for this work (solid symbols) in comparison to the work of Henshaw (Ref. 27) ($\circ, \nabla, \Delta, \square$), Mozer *et al.* (Ref. 28) ($\times, +$) and Svensson *et al.* (Ref. 29) ($\curvearrowright, \curvearrowleft, \diamond$).

maximum value of $f(k)$, f_m , is shown as a function of density. We have included in the comparison the recent work of Mozer *et al.*²⁸ and some of the saturated vapor measurements reported recently by Svensson²⁹ and co-workers. There is a general consistency among the various results but the detailed agreement is imperfect. Agreement is best between the present work and that of Mozer *et al.*²⁸ particularly for values of f_m .

Results for the pair correlation function $g(r)$ have been obtained from the liquid structure factor values through use of $S_s(k)$ and the inverse transform to

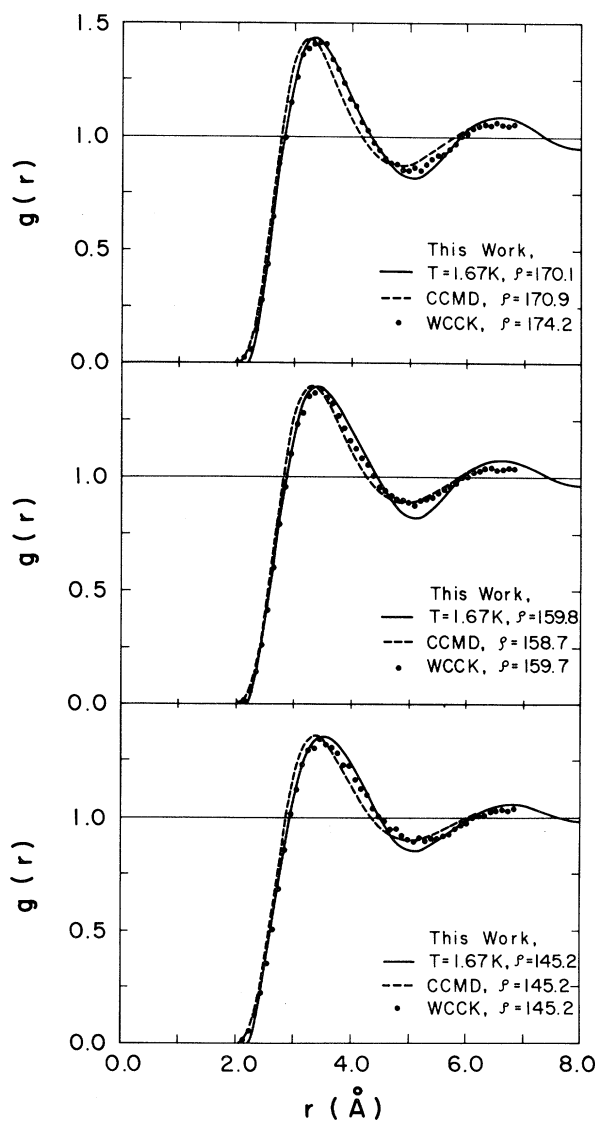


FIG. 6. The pair correlation function, $g(r)$, at 1.67 K (solid line) as determined from Fourier transform of the smoothed liquid structure factor, $S_s(k)$ (Table II). Also shown are the predictions of Chang and Campbell (Ref. 5) (dashed line) and Whitlock *et al.* (Ref. 6) (dots).

Eq. (2). $S_s(k)$ is obtained from the experimental values $S(k)$ by smoothing and interpolation to reduce the scatter in the data and provide data of regular spacing over the momentum transfer interval $0 \leq k \leq 5.1 \text{ \AA}^{-1}$. The experimental data were extrapolated smoothly to the $S(0)$ intercept during the smoothing process. Comparison is made to the work of Chang and Campbell⁵ for the Morse potential including three-body factors in Fig. 6. Also included are the Monte Carlo results of Whitlock *et al.*⁶ for the Lennard-Jones potential (dots). The data indicate a deeper first minimum in $g(r)$ than does either calculation. The position of the maximum value of the pair correlation function R_M appears to be a smooth function of density (Fig. 7) with no apparent temperature dependence. Also shown in Fig. 7 is the amplitude of the principal maximum of $g(r)$, g_m . Several values from the saturated vapor pressure measurements of Svensson *et al.*²⁹ are also shown as are the predictions of Chang and Campbell⁵ and Whitlock *et al.*⁶ The amplitude of the pair correlation function is in better agreement with the prediction of Chang and Campbell,⁵ but the position is closer to the prediction of Whitlock *et al.*⁶

Since these data were collected at fixed temperature as a function of density, isothermal density differences of the structure factor values can easily be obtained. Typical results for the extremes in density at each of the three temperatures studied are shown in Fig. 8. In general the results are consistent with the qualitative conclusions of Mozer *et al.*²⁸ That is, as a function of momentum transfer the density differences show first a minimum followed by a

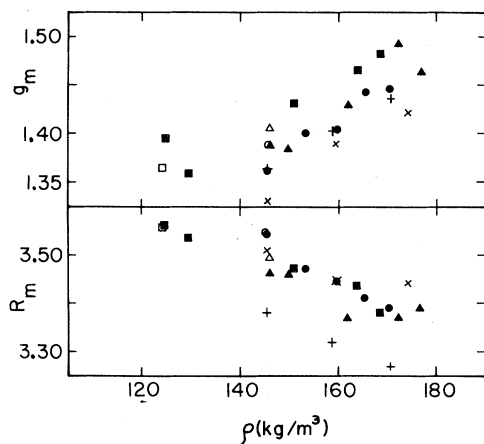


FIG. 7. The maximum value g_m and the position R_M of the main maximum of the pair correlation function as a function of the density (\bullet , 1.67 K; \blacktriangle , 2.20 K; \blacksquare , 4.24 K) for this work. Also shown are selected results from Svensson *et al.* (Ref. 29) (\circ , 1.77 K; \triangle , 2.27 K; \square , 4.27 K) and the predictions ($T=0$) of Chang and Campbell (Ref. 5) ($+$) and Whitlock *et al.* (Ref. 6) (\times).

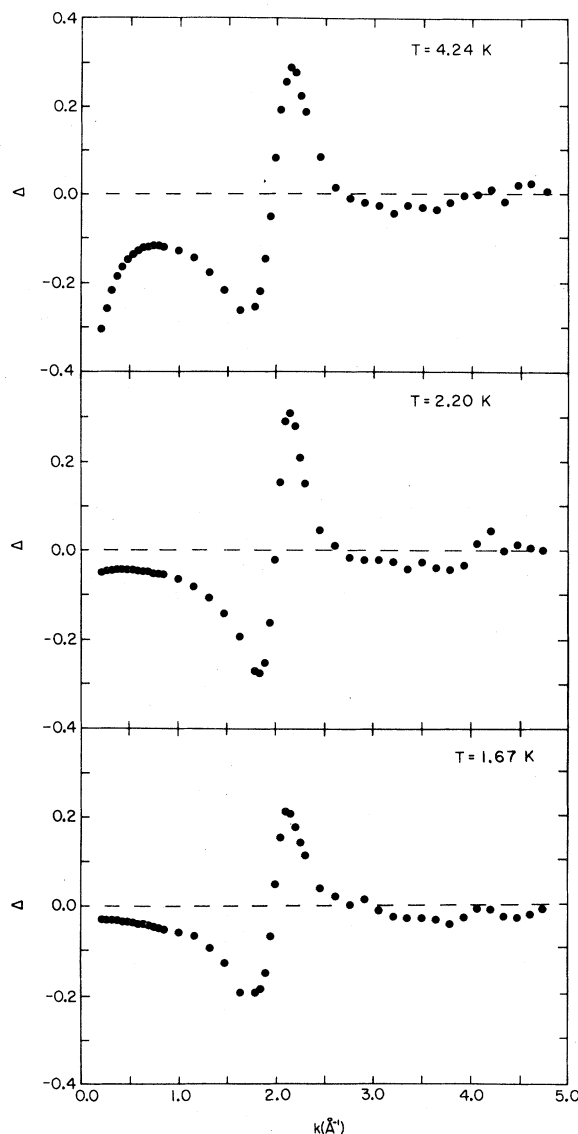


FIG. 8. Selected isothermal density differences for the three temperatures studied in this work. In each case the extremes in density values studied was used in the computation.

dramatic rise to a maximum. The data at 4.24 K show pronounced structure at small momentum transfer due to compressibility effects [Eq. (3)].

A very limited amount of constant density data ($\rho = 170.1 \text{ kg/m}^3$) was collected during this work and supports the conclusion that there is a loss in spatial order on cooling through the λ transition.^{3,4,27,28} Figure 9 shows the evolution of the height of the main structure factor maximum as a function of temperature. The behavior is similar to that seen earlier³ at saturated vapor pressure and the constant density $\rho = 150.3$ and 162.5 kg/m^3 although in the present

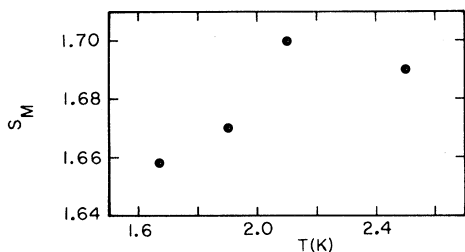


FIG. 9. Height of the principal maximum of the liquid structure factor at $\rho = 170.1 \text{ kg/m}^3$ as a function of temperature. These data are consistent with other data (Refs. 3, 4, 27, and 28) which confirm a loss of spatial order in ^4He on cooling through T .

case there is a smaller number of temperatures studied. More extensive recent work^{30,31} at $\rho = 171.0 \text{ kg m}^3$ is generally consistent with these conclusions and can be compared in detail to the predictions of Gaglione *et al.*⁷

V. SUMMARY

We have reported systematic measurements of the structure factor of ^4He at several temperatures as a function of density. Comparison has been made to the predictions of Chang and Campbell⁵ and Whitlock *et al.*⁶ both for the liquid structure factor and the pair correlation function. Comparison is also made to previous work by others and comparison is most favorable in the case of the data of Mozer *et al.*²⁸

ACKNOWLEDGMENTS

This work was supported by the National Science Foundation through Grants No. DMR77-07727 and No. DMR79-09248. We are grateful to B. L. Weiss for assistance with the digital control system and to D. A. Ewen for help with the data manipulation. We also acknowledge a grant of computer time from the University Computer Center.

APPENDIX A

In this Appendix we collect all of the tables of data resulting from the work presented here. The structure factor values $S(k)$ directly obtained from the experiments are presented in Table I. These data have not been smoothed in any way. In Table II we present smoothed structure factor values $S_s(k)$. For

these values scatter in the data have been removed by a smoothing procedure and the small momentum transfer data have been smoothly extrapolated to the intercept given by Eq. (3). In Table III we present the pair correlation function which results from a Fourier transform of the smoothed data presented in Table II. Spurious oscillations for coordinate values below the first zero r_c in $g(r)$ have been truncated from the table.

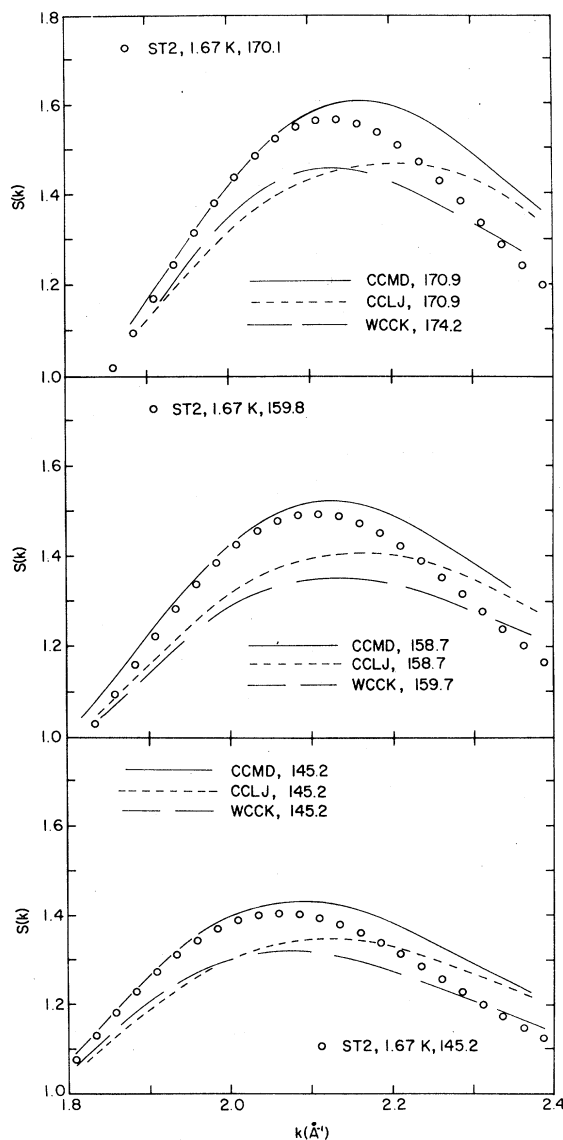


FIG. 10. Liquid structure function $S_{T_2}(k)$ in the vicinity of the principal maximum (see also Fig. 3).

TABLE I. Structure factor values $S(k)$ as obtained directly from the analysis discussed in this work. No smoothing of any kind has been applied to the data.

k (\AA^{-1})	$S(k)$ $T=1.67$ K				
	145.2	153.4	159.8	165.3	170.1
0.213	0.086	0.074	0.066	0.061	0.058
0.267	0.095	0.084	0.074	0.071	0.066
0.320	0.102	0.091	0.083	0.076	0.073
0.373	0.111	0.100	0.092	0.087	0.082
0.427	0.123	0.111	0.101	0.095	0.090
0.480	0.131	0.119	0.109	0.103	0.098
0.533	0.141	0.129	0.118	0.113	0.106
0.586	0.153	0.140	0.128	0.123	0.115
0.640	0.162	0.149	0.138	0.132	0.125
0.693	0.175	0.162	0.149	0.138	0.134
0.746	0.187	0.172	0.159	0.150	0.143
0.799	0.201	0.184	0.169	0.164	0.154
0.852	0.215	0.197	0.183	0.173	0.165
1.011	0.263	0.246	0.229	0.217	0.207
1.169	0.323	0.308	0.279	0.266	0.258
1.328	0.422	0.390	0.361	0.345	0.330
1.485	0.559	0.512	0.484	0.453	0.434
1.642	0.770	0.677	0.660	0.620	0.577
1.799	1.063	1.017	0.959	0.902	0.870
1.851	1.182	1.151	1.096	1.036	0.998
1.903	1.318	1.301	1.245	1.216	1.170
1.955	1.397	1.405	1.380	1.352	1.332
2.006	1.431	1.470	1.475	1.479	1.483
2.058	1.449	1.522	1.551	1.572	1.606
2.109	1.443	1.506	1.551	1.604	1.658
2.161	1.403	1.473	1.507	1.547	1.614
2.212	1.342	1.395	1.435	1.481	1.522
2.264	1.283	1.332	1.354	1.405	1.429
2.315	1.226	1.274	1.288	1.325	1.343
2.468	1.098	1.134	1.111	1.130	1.141
2.620	1.014	1.040	1.012	1.041	1.039
2.771	0.961	0.983	0.962	0.975	0.966
2.921	0.942	0.988	0.961	0.956	0.960
3.068	0.942	0.966	0.940	0.919	0.935
3.217	0.945	0.961	0.939	0.943	0.923
3.364	0.942	0.954	0.935	0.938	0.918
3.509	0.985	0.984	0.956	0.962	0.961
3.653	0.980	0.999	0.950	1.018	0.952
3.795	0.980	0.981	0.932	0.986	0.942
3.936	0.983	1.003	0.967	1.003	0.960
4.075	1.051	1.040	1.032	1.085	1.048
4.213	0.968	0.989	0.973	1.015	0.963
4.349	0.969	0.983	0.971	0.970	0.948
4.484	1.037	1.041	1.043	1.076	1.014
4.617	0.975	0.983	1.007	0.970	0.959
4.748	1.014	0.999	1.017	1.004	1.010
4.877	1.066	1.033	1.061	1.016	1.017
5.004	0.959	0.992	0.989	1.041	1.000
5.129	0.990	1.008	0.977	0.978	1.026

TABLE I (Continued).

k (\AA^{-1})	$S(k)$ $T=2.20$ K				
	146.1	149.9	161.8	172.2	176.6
0.213	0.106	0.094	0.075	0.062	0.058
0.267	0.111	0.101	0.080	0.069	0.066
0.320	0.115	0.105	0.085	0.075	0.071
0.373	0.120	0.113	0.093	0.083	0.078
0.427	0.129	0.121	0.101	0.091	0.058
0.480	0.136	0.127	0.108	0.098	0.094
0.533	0.144	0.135	0.118	0.106	0.101
0.586	0.155	0.147	0.127	0.115	0.110
0.640	0.163	0.155	0.136	0.123	0.117
0.693	0.174	0.168	0.145	0.131	0.128
0.746	0.185	0.176	0.152	0.141	0.134
0.799	0.195	0.187	0.162	0.151	0.143
0.852	0.210	0.205	0.177	0.162	0.157
1.011	0.257	0.248	0.218	0.202	0.194
1.169	0.321	0.308	0.274	0.250	0.240
1.328	0.408	0.389	0.344	0.316	0.302
1.485	0.539	0.512	0.454	0.418	0.398
1.642	0.740	0.672	0.588	0.571	0.547
1.799	1.060	1.031	0.915	0.827	0.791
1.851	1.190	1.167	1.063	0.966	0.916
1.903	1.346	1.315	1.238	1.138	1.095
1.955	1.435	1.432	1.402	1.322	1.273
2.006	1.491	1.500	1.525	1.504	1.471
2.058	1.522	1.518	1.613	1.679	1.676
2.109	1.489	1.494	1.628	1.757	1.779
2.161	1.436	1.437	1.552	1.730	1.744
2.212	1.360	1.367	1.463	1.610	1.638
2.264	1.290	1.295	1.368	1.483	1.499
2.315	1.238	1.232	1.288	1.385	1.389
2.468	1.084	1.099	1.108	1.142	1.130
2.620	1.011	1.033	1.015	1.027	1.023
2.771	0.960	0.983	0.960	0.965	0.945
2.921	0.963	1.001	0.957	0.954	0.943
3.070	0.941	0.975	0.949	0.935	0.921
3.217	0.948	0.967	0.926	0.941	0.924
3.364	0.948	0.938	0.920	0.919	0.908
3.509	0.987	1.016	0.940	0.974	0.963
3.653	0.974	0.976	0.929	0.960	0.937
3.795	0.958	0.945	0.924	0.960	0.916
3.936	0.980	0.974	0.950	0.986	0.949
4.075	1.023	1.045	1.041	1.040	1.041
4.213	0.956	0.984	0.963	0.991	1.002
4.349	0.944	0.975	0.942	0.979	0.945
4.484	1.037	1.031	1.015	1.064	1.052
4.617	0.992	1.009	1.007	0.997	1.000
4.748	1.011	0.982	1.045	1.015	1.014
4.877	1.006	1.014	0.995	1.020	0.985
5.004	0.963	0.960	0.973	0.999	0.976
5.129	1.027	1.037	0.975	0.970	1.023

TABLE I (Continued).

k (\AA^{-1})	$S(k)$ $T=4.24$ K				
	124.8	129.5	150.8	163.6	168.4
0.213	0.398	0.310	0.148	0.104	0.093
0.267	0.355	0.285	0.147	0.106	0.097
0.320	0.314	0.261	0.146	0.106	0.098
0.373	0.289	0.246	0.147	0.112	0.103
0.427	0.274	0.239	0.149	0.117	0.110
0.480	0.261	0.231	0.142	0.121	0.113
0.533	0.256	0.229	0.160	0.128	0.120
0.586	0.256	0.234	0.166	0.136	0.129
0.640	0.257	0.232	0.172	0.144	0.136
0.693	0.262	0.241	0.182	0.152	0.143
0.746	0.267	0.247	0.191	0.160	0.151
0.799	0.277	0.258	0.200	0.168	0.161
0.852	0.290	0.271	0.213	0.181	0.171
1.011	0.341	0.325	0.261	0.224	0.213
1.169	0.408	0.385	0.317	0.277	0.264
1.328	0.508	0.489	0.401	0.349	0.332
1.485	0.651	0.628	0.526	0.459	0.435
1.642	0.864	0.844	0.723	0.631	0.602
1.799	1.117	1.108	1.013	0.903	0.863
1.851	1.219	1.197	1.137	1.031	1.000
1.903	1.307	1.305	1.278	1.195	1.161
1.955	1.355	1.360	1.379	1.324	1.304
2.006	1.363	1.379	1.462	1.445	1.445
2.058	1.379	1.408	1.518	1.555	1.572
2.109	1.381	1.400	1.530	1.606	1.635
2.161	1.346	1.363	1.502	1.592	1.633
2.212	1.293	1.303	1.433	1.525	1.569
2.264	1.255	1.255	1.358	1.442	1.479
2.315	1.215	1.208	1.306	1.363	1.402
2.468	1.075	1.083	1.120	1.146	1.159
2.620	1.024	1.051	1.039	1.035	1.039
2.771	0.977	0.977	0.976	0.963	0.967
2.921	0.984	0.996	0.973	0.958	0.965
3.070	0.960	0.972	0.954	0.940	0.934
3.217	0.971	0.965	0.967	0.936	0.927
3.364	0.961	0.965	0.946	0.932	0.935
3.509	0.998	0.997	1.005	0.982	0.968
3.653	1.001	1.006	1.015	0.986	0.966
3.795	0.994	0.993	0.997	0.997	0.975
3.936	1.041	1.015	1.035	1.025	1.038
4.075	1.055	1.053	1.062	1.033	1.054
4.213	0.983	0.958	0.999	0.997	0.994
4.349	0.989	0.929	0.968	0.962	0.971
4.484	1.034	1.042	1.080	1.036	1.055
4.617	1.007	1.004	0.995	0.978	1.032
4.784	0.987	0.994	1.005	1.002	0.995
4.877	1.000	0.988	0.992	1.032	1.091
5.004	1.005	0.986	0.972	0.950	0.962
5.129	1.006	1.022	1.035	1.036	0.991

TABLE II. Smoothed structure factor values $S_s(k)$.

k (\AA^{-1})	$S_s(k)$, $T=1.67$ K				
	145.2	153.4	159.8	165.3	170.1
0.000	0.064	0.048	0.040	0.035	0.032
0.100	0.065	0.056	0.044	0.042	0.040
0.200	0.083	0.074	0.060	0.056	0.055
0.300	0.097	0.088	0.074	0.072	0.070
0.400	0.117	0.104	0.092	0.089	0.086
0.500	0.132	0.120	0.112	0.107	0.100
0.600	0.153	0.138	0.130	0.123	0.116
0.700	0.175	0.158	0.151	0.142	0.132
0.800	0.199	0.180	0.174	0.164	0.152
0.900	0.227	0.204	0.198	0.188	0.177
1.000	0.263	0.236	0.225	0.219	0.204
1.100	0.301	0.269	0.257	0.250	0.235
1.200	0.349	0.312	0.294	0.286	0.272
1.300	0.408	0.370	0.343	0.327	0.318
1.400	0.478	0.436	0.411	0.389	0.374
1.500	0.575	0.519	0.497	0.468	0.448
1.600	0.692	0.622	0.602	0.571	0.543
1.700	0.867	0.760	0.728	0.697	0.664
1.800	1.068	0.986	0.936	0.907	0.860
1.900	1.302	1.282	1.229	1.209	1.145
2.000	1.442	1.460	1.475	1.493	1.480
2.100	1.449	1.511	1.554	1.597	1.659
2.200	1.348	1.427	1.445	1.475	1.541
2.300	1.239	1.298	1.298	1.337	1.372
2.400	1.149	1.198	1.197	1.206	1.220
2.500	1.075	1.119	1.088	1.106	1.112
2.600	1.024	1.052	1.021	1.046	1.049
2.700	0.981	1.017	0.984	1.001	1.004
2.800	0.957	0.994	0.962	0.967	0.973
2.900	0.946	0.978	0.950	0.949	0.953
3.000	0.939	0.968	0.944	0.940	0.942
3.100	0.939	0.963	0.941	0.937	0.931
3.200	0.941	0.961	0.940	0.940	0.924
3.300	0.945	0.960	0.942	0.945	0.924
3.400	0.953	0.962	0.943	0.952	0.925
3.500	0.961	0.966	0.946	0.961	0.932
3.600	0.967	0.974	0.953	0.972	0.937
3.700	0.974	0.978	0.960	0.986	0.947
3.800	0.980	0.984	0.965	0.995	0.955
3.900	0.985	0.994	0.971	1.009	0.967
4.000	0.990	0.998	0.983	1.018	0.980
4.100	0.993	0.999	0.991	1.027	0.992
4.200	0.998	1.007	0.999	1.031	1.000
4.300	1.004	1.009	1.009	1.035	1.007
4.400	1.006	1.012	1.012	1.037	1.010
4.500	1.010	1.013	1.017	1.039	1.014
4.600	1.014	1.014	1.019	1.039	1.016
4.700	1.017	1.014	1.016	1.039	1.016
4.800	1.018	1.014	1.015	1.037	1.014
4.900	1.017	1.011	1.010	1.029	1.009
5.000	1.017	1.006	1.006	1.023	1.006

TABLE II (Continued).

k (\AA^{-1})	$S_s(k)$ $T=2.20$ K				
	146.1	149.9	161.8	172.2	176.6
0.000	0.100	0.077	0.049	0.039	0.035
0.100	0.093	0.078	0.058	0.046	0.037
0.200	0.103	0.093	0.071	0.059	0.054
0.300	0.113	0.104	0.086	0.077	0.069
0.400	0.125	0.119	0.101	0.094	0.082
0.500	0.141	0.134	0.116	0.107	0.095
0.600	0.158	0.148	0.129	0.120	0.111
0.700	0.177	0.165	0.147	0.136	0.128
0.800	0.198	0.187	0.166	0.155	0.150
0.900	0.224	0.213	0.188	0.174	0.174
1.000	0.253	0.245	0.216	0.197	0.196
1.100	0.291	0.278	0.253	0.223	0.221
1.200	0.335	0.316	0.295	0.257	0.250
1.300	0.391	0.372	0.342	0.304	0.286
1.400	0.451	0.446	0.399	0.360	0.341
1.500	0.547	0.526	0.467	0.436	0.414
1.600	0.672	0.624	0.548	0.527	0.522
1.700	0.834	0.778	0.687	0.655	0.640
1.800	1.050	1.038	0.902	0.848	0.806
1.900	1.327	1.309	1.221	1.130	1.102
2.000	1.491	1.494	1.500	1.467	1.464
2.100	1.500	1.498	1.633	1.750	1.766
2.200	1.373	1.370	1.474	1.656	1.645
2.300	1.248	1.251	1.319	1.428	1.405
2.400	1.150	1.151	1.172	1.258	1.208
2.500	1.063	1.085	1.086	1.116	1.105
2.600	1.015	1.042	1.023	1.041	1.030
2.700	0.985	1.007	0.994	1.000	0.991
2.800	0.964	0.984	0.976	0.976	0.961
2.900	0.947	0.972	0.963	0.960	0.941
3.000	0.942	0.965	0.955	0.946	0.928
3.100	0.940	0.960	0.946	0.939	0.924
3.200	0.938	0.955	0.942	0.936	0.924
3.300	0.938	0.955	0.936	0.937	0.926
3.400	0.940	0.954	0.932	0.941	0.930
3.500	0.944	0.955	0.933	0.945	0.936
3.600	0.951	0.959	0.933	0.952	0.943
3.700	0.958	0.962	0.939	0.959	0.948
3.800	0.967	0.969	0.947	0.967	0.954
3.900	0.976	0.976	0.957	0.978	0.964
4.000	0.987	0.985	0.970	0.992	0.975
4.100	0.993	0.995	0.986	1.001	0.984
4.200	1.000	1.000	1.000	1.012	0.994
4.300	1.005	1.003	1.006	1.021	1.002
4.400	1.013	1.007	1.011	1.027	1.009
4.500	1.016	1.010	1.015	1.025	1.011
4.600	1.018	1.010	1.017	1.025	1.015
4.700	1.020	1.009	1.015	1.023	1.011
4.800	1.019	1.007	1.009	1.016	1.008
4.900	1.016	1.004	1.003	1.010	1.005
5.000	1.010	1.002	0.991	1.001	1.001

TABLE II (Continued).

k (\AA^{-1})	$S_s(k)$, $T = 4.24$ K				
	124.8	129.5	150.8	163.6	168.4
0.000	0.640	0.431	0.138	0.089	0.080
0.100	0.526	0.388	0.139	0.093	0.081
0.200	0.412	0.326	0.141	0.101	0.087
0.300	0.333	0.283	0.142	0.107	0.096
0.400	0.282	0.253	0.146	0.114	0.106
0.500	0.259	0.241	0.154	0.124	0.115
0.600	0.255	0.243	0.169	0.140	0.133
0.700	0.264	0.254	0.182	0.156	0.145
0.800	0.278	0.274	0.198	0.171	0.161
0.900	0.305	0.299	0.226	0.195	0.183
1.000	0.336	0.329	0.257	0.224	0.209
1.100	0.373	0.365	0.294	0.253	0.235
1.200	0.422	0.416	0.337	0.285	0.275
1.300	0.486	0.480	0.387	0.336	0.321
1.400	0.573	0.564	0.457	0.398	0.376
1.500	0.672	0.668	0.537	0.478	0.459
1.600	0.801	0.794	0.661	0.596	0.557
1.700	0.955	0.936	0.811	0.740	0.707
1.800	1.113	1.107	1.017	0.924	0.876
1.900	1.296	1.291	1.284	1.175	1.171
2.000	1.379	1.389	1.451	1.425	1.426
2.100	1.390	1.415	1.531	1.604	1.627
2.200	1.315	1.340	1.450	1.536	1.592
2.300	1.226	1.235	1.322	1.391	1.433
2.400	1.132	1.147	1.194	1.228	1.275
2.500	1.068	1.095	1.104	1.120	1.132
2.600	1.031	1.059	1.053	1.043	1.062
2.700	1.000	1.034	1.011	0.993	1.015
2.800	0.979	1.010	0.986	0.964	0.981
2.900	0.972	0.996	0.970	0.952	0.959
3.000	0.967	0.986	0.957	0.945	0.945
3.100	0.964	0.979	0.955	0.942	0.937
3.200	0.963	0.977	0.955	0.942	0.935
3.300	0.964	0.977	0.957	0.944	0.936
3.400	0.969	0.977	0.962	0.956	0.946
3.500	0.973	0.980	0.968	0.966	0.953
3.600	0.981	0.983	0.979	0.975	0.965
3.700	0.987	0.986	0.990	0.989	0.977
3.800	0.992	0.992	0.997	0.998	0.986
3.900	0.997	0.995	1.004	1.005	0.998
4.000	1.002	1.001	1.013	1.011	1.009
4.100	1.002	1.002	1.014	1.016	1.014
4.200	1.007	1.004	1.019	1.018	1.022
4.300	1.009	1.004	1.018	1.020	1.023
4.400	1.006	1.004	1.018	1.020	1.024
4.500	1.004	1.004	1.018	1.020	1.026
4.600	1.001	1.007	1.018	1.019	1.026
4.700	0.999	1.006	1.015	1.017	1.026
4.800	0.999	1.006	1.012	1.013	1.022
4.900	0.996	1.004	1.010	1.007	1.015
5.000	0.996	1.002	1.005	1.000	1.010

TABLE III. Values for the pair correlation function $g(r)$ which result from a Fourier transform of the smoothed structure factor $S_g(k)$ presented in Table II.

r (Å)	$g(r)$					$T = 1.67$ K					
	145.2	153.4	159.8	163.5	170.1	r (Å)	145.2	153.4	159.8	163.5	170.1
2.200	0.000	0.000	0.000	0.000	0.000	7.400	1.023	1.018	1.012	1.008	1.003
2.300	0.018	0.085	0.073	0.051	0.071	7.500	1.014	1.006	0.999	0.995	0.989
2.400	0.149	0.225	0.213	0.172	0.225	7.600	1.007	0.996	0.988	0.985	0.977
2.500	0.307	0.385	0.376	0.329	0.403	7.700	1.000	0.987	0.978	0.976	0.966
2.600	0.479	0.555	0.553	0.512	0.594	7.800	0.994	0.979	0.970	0.970	0.958
2.700	0.654	0.727	0.732	0.706	0.783	7.900	0.989	0.974	0.965	0.965	0.953
2.800	0.820	0.891	0.902	0.896	0.962	8.000	0.983	0.969	0.961	0.962	0.950
2.900	0.969	1.039	1.055	1.068	1.118	8.100	0.978	0.966	0.960	0.960	0.949
3.000	1.095	1.164	1.182	1.212	1.247	8.200	0.974	0.965	0.960	0.959	0.950
3.100	1.194	1.262	1.280	1.321	1.343	8.300	0.972	0.965	0.961	0.959	0.953
3.200	1.268	1.333	1.349	1.394	1.406	8.400	0.970	0.965	0.964	0.960	0.957
3.300	1.317	1.377	1.388	1.433	1.439	8.500	0.970	0.967	0.967	0.963	0.963
3.400	1.347	1.397	1.403	1.442	1.444	8.600	0.972	0.970	0.972	0.967	0.970
3.500	1.359	1.397	1.397	1.427	1.428	8.700	0.975	0.974	0.977	0.973	0.977
3.600	1.359	1.380	1.377	1.397	1.396	8.800	0.979	0.979	0.983	0.980	0.986
3.700	1.348	1.352	1.346	1.357	1.353	8.900	0.984	0.984	0.990	0.987	0.994
3.800	1.327	1.315	1.308	1.311	1.303	9.000	0.989	0.990	0.996	0.995	1.003
3.900	1.299	1.272	1.266	1.262	1.250	9.100	0.993	0.996	1.002	1.003	1.010
4.000	1.262	1.225	1.221	1.212	1.196	9.200	0.997	1.002	1.008	1.010	1.017
4.100	1.219	1.176	1.175	1.162	1.143	9.300	1.001	1.007	1.013	1.016	1.023
4.200	1.170	1.126	1.127	1.110	1.090	9.400	1.004	1.011	1.017	1.020	1.027
4.300	1.116	1.076	1.079	1.059	1.039	9.500	1.006	1.014	1.020	1.023	1.030
4.400	1.062	1.027	1.031	1.008	0.991	9.600	1.008	1.017	1.021	1.024	1.031
4.500	1.008	0.981	0.983	0.958	0.946	9.700	1.009	1.018	1.022	1.024	1.030
4.600	0.960	0.939	0.938	0.913	0.905	9.800	1.011	1.018	1.021	1.024	1.028
4.700	0.918	0.903	0.898	0.874	0.870	9.900	1.012	1.018	1.020	1.022	1.025
4.800	0.886	0.873	0.864	0.844	0.843	10.000	1.013	1.018	1.018	1.020	1.021
4.900	0.864	0.852	0.838	0.924	0.823	10.100	1.014	1.016	1.016	1.018	1.017
5.000	0.852	0.840	0.822	0.815	0.813	10.200	1.014	1.015	1.013	1.016	0.013
5.100	0.850	0.836	0.817	0.816	0.812	10.300	1.013	1.013	1.011	1.013	1.008
5.200	0.855	0.840	0.821	0.826	0.820	10.400	1.012	1.011	1.008	1.009	1.003
5.300	0.865	0.850	0.834	0.844	0.836	10.500	1.010	1.008	1.005	1.005	0.999
5.400	0.879	0.866	0.854	0.866	0.857	10.600	1.007	1.006	1.002	1.001	0.995
5.500	0.894	0.886	0.879	0.891	0.884	10.700	1.005	1.003	1.000	0.997	0.992
5.600	0.911	0.908	0.907	0.917	0.913	10.800	1.002	1.000	0.997	0.994	0.989
5.700	0.927	0.931	0.935	0.942	0.943	10.900	0.999	0.998	0.994	0.990	0.986
5.800	0.943	0.954	0.963	0.966	0.972	11.000	0.997	0.995	0.992	0.988	0.984
5.900	0.960	0.976	0.989	0.988	0.999	11.100	0.996	0.993	0.990	0.986	0.983
6.000	0.976	0.996	1.011	1.009	1.024	11.200	0.995	0.991	0.988	0.985	0.983
6.100	0.993	1.015	1.031	1.027	1.046	11.300	0.994	0.990	0.987	0.985	0.983
6.200	1.010	1.032	1.047	1.045	1.064	11.400	0.994	0.990	0.987	0.985	0.984
6.300	1.026	1.046	1.059	1.060	1.078	11.500	0.993	0.990	0.988	0.987	0.986
6.400	1.040	1.058	1.069	1.072	1.088	11.600	0.993	0.990	0.988	0.988	0.988
6.500	1.051	1.067	1.075	1.082	1.093	11.700	0.993	0.991	0.990	0.990	0.990
6.600	1.060	1.073	1.079	1.087	1.095	11.800	0.993	0.992	0.992	0.992	0.993
6.700	1.064	1.075	1.079	1.088	1.093	11.900	0.993	0.993	0.993	0.994	0.996
6.800	1.065	1.074	1.076	1.085	1.086	12.000	0.993	0.994	0.995	0.996	0.999
6.900	1.062	1.070	1.070	1.077	1.077	12.100	0.994	0.995	0.997	0.998	1.002
7.000	1.057	1.063	1.062	1.066	1.065	12.200	0.995	0.997	0.999	1.000	1.004
7.100	1.049	1.053	1.051	1.052	1.050	12.300	0.997	0.998	1.000	1.002	1.006
7.200	1.040	1.042	1.039	1.037	1.035	12.400	0.998	0.999	1.002	1.004	1.008
7.300	1.031	1.030	1.025	1.022	1.019	12.500	1.000	1.000	1.003	1.006	1.010

TABLE III (Continued).

r (Å)	$g(r)$					$T = 2.20$ K					
	146.1	149.9	161.8	172.2	176.6	r (Å)	146.1	149.9	161.8	172.2	176.6
2.200	0.000	0.000	0.000	0.000	0.002	7.400	1.028	1.031	1.017	0.995	1.000
2.300	0.003	0.072	0.071	0.058	0.095	7.500	1.016	1.019	1.000	0.978	0.983
2.400	0.117	0.212	0.221	0.202	0.247	7.600	1.005	1.008	0.984	0.963	0.969
2.500	0.283	0.371	0.392	0.374	0.419	7.700	0.995	0.997	0.971	0.951	0.956
2.600	0.467	0.540	0.575	0.563	0.603	7.800	0.987	0.988	0.961	0.943	0.947
2.700	0.656	0.709	0.758	0.757	0.786	7.900	0.981	0.980	0.954	0.938	0.941
2.800	0.836	0.871	0.933	0.945	0.959	8.000	0.976	0.974	0.950	0.937	0.938
2.900	0.998	1.017	1.089	1.115	1.114	8.100	0.971	0.969	0.948	0.939	0.938
3.000	1.134	1.141	1.219	1.258	1.243	8.200	0.968	0.965	0.949	0.943	0.941
3.100	1.240	1.240	1.318	1.368	1.342	8.300	0.966	0.963	0.952	0.950	0.946
3.200	1.315	1.311	1.385	1.442	1.411	8.400	0.965	0.962	0.955	0.957	0.953
3.300	1.361	1.357	1.421	1.482	1.449	8.500	0.966	0.963	0.959	0.965	0.961
3.400	1.383	1.379	1.428	1.490	1.461	8.600	0.967	0.964	0.964	0.974	0.970
3.500	1.386	1.382	1.413	1.471	1.450	8.700	0.970	0.967	0.970	0.983	0.980
3.600	1.374	1.368	1.382	1.433	1.421	8.800	0.974	0.971	0.976	0.992	0.991
3.700	1.352	1.344	1.341	1.382	1.379	8.900	0.979	0.976	0.983	1.002	1.001
3.800	1.323	1.311	1.294	1.324	1.328	9.000	0.984	0.982	0.992	1.001	1.010
3.900	1.290	1.273	1.247	1.264	1.272	9.100	0.990	0.988	1.000	1.019	1.019
4.000	1.253	1.233	1.201	1.203	1.213	9.200	0.996	0.995	1.009	1.027	1.027
4.100	1.213	1.190	1.157	1.145	1.154	9.300	1.002	1.001	1.017	1.033	1.033
4.200	1.169	1.147	1.115	1.090	1.096	9.400	1.007	1.007	1.024	1.037	1.037
4.300	1.123	1.103	1.075	1.037	1.039	9.500	1.011	1.012	1.028	1.039	1.039
4.400	1.074	1.059	1.033	0.987	0.985	9.600	1.014	1.016	1.031	1.038	1.039
4.500	1.024	1.016	0.992	0.940	0.935	9.700	1.016	1.019	1.032	1.036	1.038
4.600	0.976	0.974	0.950	0.896	0.890	9.800	1.017	1.020	1.030	1.031	1.034
4.700	0.932	0.935	0.909	0.857	0.851	9.900	1.018	1.021	1.027	1.026	1.030
4.800	0.894	0.901	0.871	0.824	0.821	10.000	1.018	1.021	1.023	1.019	1.024
4.900	0.864	0.872	0.839	0.800	0.799	10.100	1.017	1.020	1.019	1.013	1.017
5.000	0.843	0.851	0.815	0.786	0.788	10.200	1.016	1.019	1.015	1.007	1.011
5.100	0.833	0.838	0.802	0.784	0.788	10.300	1.015	1.017	1.011	1.001	1.004
5.200	0.831	0.834	0.800	0.792	0.797	10.400	1.013	1.015	1.007	0.996	0.998
5.300	0.838	0.838	0.809	0.811	0.817	10.500	1.011	1.012	1.004	0.992	0.992
5.400	0.852	0.849	0.828	0.839	0.843	10.600	1.008	1.010	1.002	0.989	0.988
5.500	0.870	0.866	0.856	0.873	0.875	10.700	1.005	1.007	0.999	0.986	0.983
5.600	0.890	0.887	0.889	0.911	0.910	10.800	1.002	1.004	0.996	0.983	0.980
5.700	0.912	0.911	0.924	0.949	0.946	10.900	0.999	1.001	0.993	0.981	0.978
5.800	0.935	0.936	0.959	0.985	0.981	11.000	0.996	0.998	0.990	0.980	0.976
5.900	0.956	0.960	0.991	1.017	1.012	11.100	0.993	0.995	0.987	0.979	0.976
6.000	0.977	0.983	1.019	1.045	1.039	11.200	0.991	0.992	0.984	0.980	0.976
6.100	0.997	1.004	1.042	1.066	1.062	11.300	0.990	0.990	0.983	0.981	0.978
6.200	1.015	1.023	1.060	1.083	1.079	11.400	0.990	0.989	0.982	0.983	0.980
6.300	1.032	1.039	1.073	1.094	1.092	11.500	0.990	0.988	0.983	0.986	0.984
6.400	1.047	1.052	1.082	1.101	1.100	11.600	0.990	0.988	0.984	0.990	0.987
6.500	1.060	1.062	1.088	1.104	1.103	11.700	0.991	0.988	0.987	0.994	0.992
6.600	1.069	1.069	1.092	1.103	1.103	11.800	0.992	0.989	0.990	0.998	0.996
6.700	1.076	1.074	1.092	1.099	1.099	11.900	0.993	0.990	0.994	1.002	1.000
6.800	1.078	1.075	1.090	1.091	1.091	12.000	0.994	0.991	0.998	1.005	1.004
6.900	1.076	1.074	1.085	1.081	1.081	12.100	0.995	0.993	1.001	1.008	1.008
7.000	1.071	1.069	1.076	1.067	1.067	12.200	0.996	0.994	1.003	1.010	1.011
7.100	1.063	1.062	1.065	1.051	1.052	12.300	0.998	0.996	1.005	1.011	1.013
7.200	1.052	1.053	1.051	1.033	1.035	12.400	0.999	0.998	1.006	1.011	1.015
7.300	1.040	1.042	1.034	1.014	1.017	12.500	1.000	1.000	1.006	1.011	1.016

TABLE III (Continued).

r (Å)	$g(r)$					$T=4.24$ K					
	124.8	129.5	150.8	163.6	168.4	r (Å)	124.8	129.5	150.8	163.6	168.4
2.200	0.000	0.000	0.000	0.009	0.000	7.400	1.028	1.023	1.016	1.001	0.994
2.300	0.057	0.070	0.058	0.100	0.063	7.500	1.020	1.014	1.004	0.987	0.980
2.400	0.170	0.202	0.180	0.221	0.200	7.600	1.011	1.006	0.994	0.975	0.969
2.500	0.301	0.349	0.328	0.366	0.367	7.700	1.003	0.999	0.985	0.966	0.961
2.600	0.444	0.505	0.493	0.529	0.552	7.800	0.995	0.993	0.978	0.960	0.956
2.700	0.595	0.662	0.666	0.702	0.744	7.900	0.989	0.988	0.972	0.956	0.953
2.800	0.747	0.813	0.838	0.874	0.931	8.000	0.984	0.984	0.968	0.956	0.953
2.900	0.893	0.952	0.998	1.035	1.101	8.100	0.981	0.981	0.966	0.957	0.955
3.000	1.028	1.074	1.138	1.178	1.244	8.200	0.979	0.979	0.965	0.960	0.958
3.100	1.146	1.175	1.253	1.294	1.355	8.300	0.978	0.977	0.966	0.965	0.962
3.200	1.243	1.253	1.339	1.381	1.430	8.400	0.979	0.976	0.968	0.970	0.967
3.300	1.317	1.308	1.396	1.437	1.471	8.500	0.980	0.977	0.970	0.976	0.973
3.400	1.365	1.342	1.424	1.462	1.480	8.600	0.982	0.978	0.974	0.981	0.980
3.500	1.390	1.357	1.428	1.460	1.464	8.700	0.985	0.980	0.978	0.988	0.987
3.600	1.392	1.355	1.412	1.435	1.427	8.800	0.987	0.983	0.983	0.994	0.994
3.700	1.377	1.340	1.380	1.394	1.378	8.900	0.990	0.987	0.989	1.000	1.001
3.800	1.347	1.315	1.337	1.341	1.320	9.000	0.993	0.991	0.994	1.005	1.008
3.900	1.308	1.282	1.287	1.281	1.259	9.100	0.996	0.996	1.000	1.011	1.015
4.000	1.262	1.244	1.234	1.218	1.197	9.200	0.999	1.001	1.005	1.015	1.020
4.100	1.215	1.202	1.179	1.156	1.137	9.300	1.002	1.005	1.009	1.019	1.024
4.200	1.167	1.159	1.125	1.096	1.079	9.400	1.005	1.009	1.013	1.022	1.027
4.300	1.121	1.115	1.073	1.039	1.025	9.500	1.008	1.012	1.015	1.023	1.028
4.400	1.078	1.072	1.024	0.988	0.974	9.600	1.009	1.014	1.017	1.023	1.027
4.500	1.038	1.031	0.979	0.942	0.928	9.700	1.011	1.015	1.018	1.022	1.025
4.600	1.002	0.993	0.939	0.902	0.888	9.800	1.012	1.015	1.018	1.020	1.022
4.700	0.970	0.960	0.905	0.869	0.855	9.900	1.012	1.015	1.017	1.017	1.017
4.800	0.942	0.931	0.877	0.843	0.831	10.000	1.011	1.014	1.015	1.013	1.013
4.900	0.918	0.909	0.857	0.826	0.815	10.100	1.011	1.012	1.013	1.009	1.009
5.000	0.898	0.893	0.844	0.818	0.809	10.200	1.010	1.010	1.011	1.006	1.004
5.100	0.884	0.883	0.839	0.819	0.813	10.300	1.008	1.009	1.009	1.002	1.001
5.200	0.876	0.880	0.842	0.827	0.826	10.400	1.007	1.007	1.006	0.999	0.997
5.300	0.874	0.882	0.851	0.844	0.845	10.500	1.006	1.005	1.004	0.997	0.994
5.400	0.878	0.888	0.866	0.866	0.871	10.600	1.004	1.003	1.001	0.994	0.992
5.500	0.888	0.899	0.885	0.892	0.899	10.700	1.003	1.001	0.999	0.993	0.990
5.600	0.902	0.912	0.907	0.920	0.929	10.800	1.002	0.999	0.996	0.991	0.988
5.700	0.920	0.927	0.930	0.949	0.958	10.900	1.000	0.997	0.994	0.990	0.987
5.800	0.940	0.943	0.953	0.977	0.986	11.000	0.999	0.995	0.993	0.989	0.986
5.900	0.960	0.960	0.976	1.002	1.010	11.100	0.997	0.994	0.991	0.988	0.986
6.000	0.980	0.977	0.997	1.025	1.032	11.200	0.996	0.993	0.991	0.988	0.987
6.100	0.998	0.993	1.016	1.043	1.050	11.300	0.995	0.993	0.991	0.988	0.988
6.200	1.014	1.008	1.034	1.058	1.065	11.400	0.995	0.992	0.991	0.989	0.990
6.300	1.027	1.022	1.048	1.069	1.076	11.500	0.994	0.993	0.992	0.991	0.992
6.400	1.037	1.034	1.060	1.077	1.084	11.600	0.995	0.993	0.993	0.993	0.995
6.500	1.045	1.044	1.068	1.082	1.088	11.700	0.995	0.994	0.995	0.995	0.997
6.600	1.051	1.051	1.074	1.083	1.089	11.800	0.996	0.996	0.996	0.998	1.000
6.700	1.054	1.056	1.076	1.081	1.086	11.900	0.997	0.997	0.997	1.000	1.002
6.800	1.055	1.058	1.074	1.076	1.079	12.000	0.998	0.998	0.999	1.002	1.004
6.900	1.055	1.057	1.069	1.068	1.069	12.100	0.999	0.999	1.000	1.004	1.005
7.000	1.052	1.053	1.062	1.057	1.056	12.200	1.000	1.000	1.001	1.005	1.006
7.100	1.048	1.047	1.052	1.045	1.041	12.300	1.000	1.001	1.002	1.006	1.007
7.200	1.043	1.040	1.041	1.030	1.025	12.400	1.001	1.002	1.003	1.007	1.007
7.300	1.036	1.032	1.028	1.015	1.009	12.500	1.001	1.002	1.003	1.007	1.007

APPENDIX B

In order to check on the consistency between the pair correlation function $g(r)$ and the structure factor $S_s(k)$ we have transformed $g(r)$ to get $S_T(k)$. The values of $S_T(k)$ so obtained are observed to have minor oscillations at small momentum transfer similar to those seen in our earlier work⁸ (Fig. 17 of Ref. 8) and a somewhat lower main structure factor peak. A repetition of the forward and reverse transform, again removing spurious oscillations, results in the structure factor $S_{T2}(k)$ which is quite similar to $S_{T1}(k)$. Figure 10 shows $S_{T2}(k)$ values in the vicinity of the main structure factor peak on comparison to theoretical predictions. Reference should again be made to Fig. 3 for a comparison with $S(k)$ obtained directly from the experiments with no smoothing or other manipulation.

APPENDIX C

A perfect structure factor should satisfy the sum rule

$$I = \frac{1}{2\pi^2\rho} \int_0^\infty [S(k) - 1] k^2 dk = -1 \quad (4)$$

Finite experimental data demand the integral be cut off at the largest available value for the momentum

TABLE IV. Values for the integral condition, Eq. (4), as applied to $S_s(k)$ and $S_{T2}(k)$.

$T(K)$	$\rho(\text{kg/m}^3)$	I_s	I_{T2}
1.67	145.2	-0.688	-0.691
1.67	153.4	-0.072	-0.773
1.67	159.8	-0.955	-0.733
1.67	165.3	-0.592	-0.665
1.67	170.1	-1.016	-0.709
2.20	146.1	-0.866	-0.669
2.20	149.9	-0.818	-0.781
2.20	161.8	-1.389	-0.733
2.20	172.2	-0.248	-0.671
2.20	176.6	-1.279	-0.713
4.24	124.8	-0.385	-0.777
4.24	129.5	+0.332	-0.714
4.24	150.8	+0.365	-0.703
4.24	163.6	+0.064	-0.723
4.24	168.4	+0.294	-0.644

transfer. Thus, due to the k^2 factor in the integrand one must exercise caution in the application of Eq. (4) to an actual experimental result. Nonetheless, we have applied the integral condition to the structure factors $S_s(k)$ and $S_{T2}(k)$ with the results shown in Table IV.

- ¹W. H. Keesom and K. W. Taconis, *Physica* **5**, 270 (1938).
²H. Frolich, *Physica* **4**, 639 (1937).
³H. N. Robkoff, D. A. Ewen, and R. B. Hallock, *Phys. Rev. Lett.* **43**, 2006 (1979).
⁴V. F. Sears and E. C. Svensson, *Phys. Rev. Lett.* **43**, 2009 (1979).
⁵C. C. Chang and C. E. Campbell, *Phys. Rev. B* **15**, 4238 (1977).
⁶P. A. Whitlock, D. M. Ceperley, G. V. Chester, and M. H. Kalos, *Phys. Rev. B* **19**, 5598 (1979).
⁷G. Gaglione, G. L. Masserine, and L. Reatto, *Phys. Rev. B* **23**, 1129 (1981).
⁸H. N. Robkoff and R. B. Hallock, *Phys. Rev. B* **24**, 159 (1981).
⁹H. N. Robkoff, B. L. Weiss, and R. B. Hallock, *Rev. Sci. Instrum.* **52**, 1037 (1981).
¹⁰See, for example, N. S. Gingrich, *Rev. Mod. Phys.* **15**, 40 (1943).
¹¹R. D. Murphy, *Phys. Rev. A* **5**, 331 (1972).
¹²L. R. Whitney, F. J. Pinski, and C. E. Campbell, *J. Low Temp. Phys.* **44**, 367 (1981).
¹³N. Metropolis, A. W. Rosenbluth, M. N. Rosenbluth, A. M. Teller, and E. Teller, *J. Chem. Phys.* **21**, 1087 (1953).
¹⁴Rigaku/USA, Danvers, Mass.
¹⁵Linde, high purity grade.
¹⁶Cryocal.

- ¹⁷See, for example, R. B. Hallock, *Phys. Rev. A* **5**, 320 (1972).
¹⁸The suggestion that this procedure was a useful one was first made and used a number of years ago [A. G. Tweet, *Phys. Rev.* **93**, 15 (1954).]
¹⁹Y. K. Kim and M. Inokuti, *Phys. Rev.* **165**, 39 (1967).
²⁰C. Tovar, D. Nicolas, and M. Ronault, *J. Chim. Phys.* **64**, 540 (1967).
²¹*International Tables for X-Ray Crystallography*, edited by K. Lonsdale (Kynoch, Birmingham, England, 1962).
²²D. L. Elwell and H. Meyer, *Phys. Rev.* **164**, 245 (1967).
²³J. Maynard, *Phys. Rev. B* **14**, 3868 (1976).
²⁴R. D. McCarty, *J. Phys. Chem. Ref. Data* **2**, 923 (1973).
²⁵J. H. Dymond and E. B. Smith, *The Virial Coefficients of Gases* (Oxford University Press, London, 1969).
²⁶L. Goldstein, *Phys. Rev.* **84**, 446 (1951).
²⁷D. G. Henshaw, *Phys. Rev.* **119**, 14 (1960).
²⁸B. Mozer, L. A. DeGraaf, and B. LeNeindre, *Phys. Rev. A* **9**, 448 (1974).
²⁹E. C. Svensson, V. F. Sears, A. D. B. Woods, and P. Martel, *Phys. Rev. B* **21**, 3638 (1978). See also, V. F. Sears, E. C. Svensson, A. D. B. Woods, and P. Martel (unpublished).
³⁰H. N. Robkoff, D. A. Ewen, F. Wirth, and R. B. Hallock, *Bull. Am. Phys. Soc.* **26**, 633 (1981).
³¹D. A. Ewen, F. Wirth, and R. B. Hallock (unpublished).